Total Energy Calculations for Silane Dissociative Chemisorption onto Si(100) and Si(111) Surfaces

Jyh-Shing Lin^a* (), Yu-Tzu Kuo^a (), Ji-Cheng Chen^a () and Ming-Hsien Lee^b () ^aDepartment of Chemistry, Tamkang University, Tamsui, Taiwan 25137, R.O.C. ^bDepartment of Physics, Tamkang University, Tamsui, Taiwan 25137, R.O.C.

Total energy calculations based on density functional theory in connection with generalized gradient approximation (GGA) and norm-conserving optimized pseudopotential approximation have been used to investigate the silane chemisorption onto Si(111) and Si(100) surfaces. Firstly, the calculated relaxed surface structure of Si(100)-(2×2) has a different dangling bonds environment from that of the calculated relaxed surface structure of Si(111)-(1×1). Secondly, our calculated results indicate that SiH_4 chemisorption onto both Si(100)-(2×2) and Si(111)-(1×1) surfaces are energetically favorable and they lead to the formation of SiH_3 and H adsorbed on the Si=Si dimer, i.e. Si(100)-(2×2)(SiH_3 :H) and the surface dihydride SiH_2 and 2H, i.e. Si(111)-(1×1)(SiH_2 :2H), respectively. Finally, the increase of dangling bond density and the absence of adatom backbond breaking are probably two of the key factors controlling the distinct increase in reaction probability for dissociative chemisorption of SiH_4 onto Si(111)-(7×7) due to Si(111)-(7×7) \leftrightarrow Si(111)-(1×1) phase transition at surface temperature greater than 800 °C.

INTRODUCTION

The surface chemistry of silicon 1 has begun to attract many surface scientists to investigate with the use of many modern tools. This is due to the fact that the understanding and the control of silicon surfaces and corresponding chemistry are of great importance in the silicon thin film deposition processing. 2 Normally, the silicon thin film is routinely grown from gaseous molecules in a variety of chemical vapor deposition (CVD) processes, and silane (SiH₄) is one of the most common CVD precursors for Si, SiO₂ and other materials. During the CVD growth of Si film, SiH₄ chemisorbs onto the surface of the growing film and the decomposition of surfaces SiH_x leads to film growth and H₂ as a byproduct.

The recent experimental work^{3,4} of S. M. Gates et al. regarding the observation of the silicon hydrides species formed by SiH₄ chemisorption on clean single crystal silicon surface Si(100)-(2×1) using static secondary ion mass spectrometry (SSIMS) suggests that the dissociation of SiH₄ to SiH₃ and H occurs on the Si(100)-(2×1) surface, which contains pairs of dangling bonds located on Si=Si dimers. In addition, they proposed the possible mechanisms describing SiH₄ chemisorption onto the Si(100)-(2×1) surface. They believed that two new bonds are formed to the H and SiH₃ fragments from two dangling bonds on two adjacent surface Si atoms. The two dangling bonds could be on dimerized Si atoms, or on two atoms from two adjacent dimers.

Another experimental work of M. E. Jones et al.5 em-

ploying supersonic molecular beam scattering techniques to investigate the translationally activated dissociative chemisorption of SiH₄ onto Si(111)-(7×7) surface found that a distinct increase in reaction probability is evident at surface temperature (T_s) greater than 800°C; this increase corresponds well to the Si(111)-(7×7) \leftrightarrow Si(111)-(1×1) phase transition known to occur on this surface. In consequence, the Si(111)-(1×1) is more reactive toward SiH₄ than the Si(111)-(7×7). Finally, they emphasized that both dangling bond density and surface structure influence greatly the reaction probability but without describing the possible reaction mechanisms for this enhanced reaction probability in the process of dissociative chemisorption of SiH₄ onto Si(111)-(1×1) surface.

Although many quantum mechanic cluster model studies of surface chemistry on Si surfaces have been reported, 6,7 the study of forming and breaking of covalent bonds as SiH₄ chemisorbs on the different Si surfaces is still a very challenging problem. For example, it is impossible for the finite sizes of cluster models to include the long range interaction through the whole Si surface. Also it is very difficult to treat the surface effect effectively. We therefore devote ourselves here to the ab initio determination of the extended surfaces of both Si(100) and Si(111) and their energetic of chemisorbed SiH_x (x = 4,3,2) species on both Si(100) and Si(111) surfaces in order to provide, at the atomic level, the understanding and reasoning of the process for dissociative chemisorbtion of SiH₄ onto the Si(100)-(2×1) and Si(111)-(7×7) (T_s>800 °C) surfaces as studied by S. M. Gates et al. and M. E. Jones et al., re-

spectively.

COMPUTATIONAL METHODS

Density functional theory with generalized gradient approximation (GGA) is applied to perform the ab initio total energy pseudopotential calculations.8 Our computational strategy is to perform all the calculations using periodic boundary conditions (sometimes known as the supercell method), with the electronic orbitals represented by using a plane-wave basis sets. We have used an ab initio molecular dynamic method based on the conjugated gradient technique^{9,10} to minimize the Kohn-Sham energy functional in which the GGA of Perdew and Wang¹⁸ is utilized. For the brillouin-zone integration we used a 2×2×1 grid of Monkhorst-Pack special points¹¹ after convergence test with 3×3×1 grid. Plane waves with an energy up to a cut-off of 300 eV were included in the basis sets. We also explored the plane-wave convergence tests by calculating the structural parameters of SiH₄, i.e. bond length of Si-H, and chemisorption energy of SiH₄ chemisorbed onto the Si(100) surface. Our calculated bond length of Si-H with a cut-off of 300 eV is accurate up to 0.005 Å in comparison with that with a cut-off of 400 eV and our calculated chemisorption energy of SiH₄ chemisorbed onto Si(100) with a cut-off of 400 eV is only 0.008 eV larger than that with a cut-off of 300 eV as shown in Table 1. These test results clearly indicate that the energy cut-off of 300 eV will be enough for the calculated physical properties of our interest in this study. A Kleinman-Bylander representation¹² of the pseudopotential is used. This allows the plane-wave matrix elements of the pseudopotential to be expressed in separable form for computational efficiency. In our calculations both surface model of Si(100) and

Table 1. Energy Cut-off Tests for the Bond Length of Si-H within SiH₄ and the Chemisorption Energy of SiH₄
Chemisorbed onto the Si(100)-(2×2) Surface

Energy cut-off (eV)	Si-H bond length (Å)
200	1.514
300	1.493
400	1.487
500	1.484
600	1.481
Expt.	1.4798

Energy cut-off (eV)	E _{chemisorb.} (eV)
200	1.984
300	1.966
400	1.958

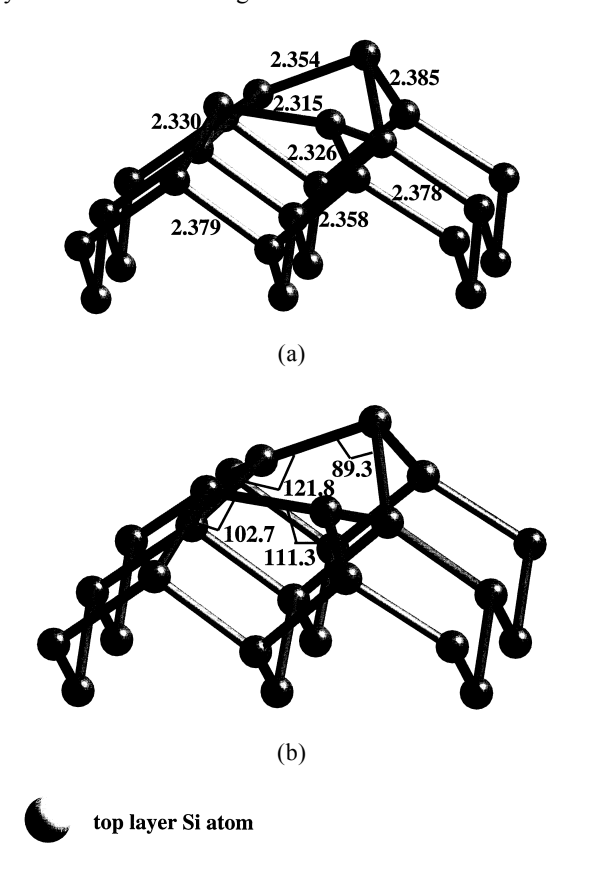
Si(111) were represented by periodically repeated slab of Si atoms (six layers in the unreconstructed geometry) with one side of three layers fixed and the other followed by a vacuum region of approximately 13 Å. These vacuum layers are mainly introduced to avoid the interaction between surfaces due to the periodicity along the [100] and [111] directions. In addition, the dangling bonds on the side of the fixed layers were passivated by H atom to eliminate the charge sloshing effect between the two surfaces. The bond lengths of Si-H are determined by optimizing all the bond lengths of Si-H with the constraint that six layers of the slab is fixed.

The pseudopotential of silicon was constructed as usual from an all-electron atomic calculation, with the condition of norm conservation and continuity of the wavefunction and its first and second derivatives at the core radius. To improve the convergence one additional requirement to those mentioned above was added, namely that the kinetic energy associated with each pseudo-wavefunction above a chosen wave vector be minimized. We have used the method of optimized pseudopotential generation, ¹³ with a reference atomic configuration of $3s^23p^2$ for s and p components and $3s^23p^{0.75}3d^{0.25}$ for the d component, and core radii of 1.80 a.u. The s-wave component was taken to be the local for the Kleinman-Bylander representation. A pure Coulomb potential is used for hydrogen throughout this study.

CALCULATED RESULTS AND DISCUSSION

Surface structure of Si(100)-(2×2)

Although many experimental efforts have been devoted to solving the question of whether the Si=Si dimers are buckled or symmetric on this particular surface, the final conclusion has not been made yet. For example, the low-temperature STM experiments demonstrated unambiguously that the Si=Si dimers at equilibrium are buckled¹⁹ and at room temperature, the Si=Si dimers appear to be symmetric because of rapid flicking between the two possible buckled orientations. In this study we first investigated the atomic arrangement of the Si(100) surface model. We assume that the Si(100) surface when being generated will convert from Si(100)- (2×1) to Si(100)- $(2\times2)^1$ during the relaxation. This surface model of Si(100)-(2×2) where the adjacent Si=Si dimers in a row buckle in an opposite direction will be used throughout this study to represent the Si(100)-(2×1) as described in the paper of S. M. Gate et al. The calculated relaxed geometry is shown in Fig. 1 and the corresponding structural parameters are reported. The reconstruction of the clean Si(100) surface gives rise to the formation of buckled Si=Si dimers with bond lengths of 2.315 Å and 2.354 Å, respectively, and which are about 0.10 Å larger than the bond length of the Si=Si double bond in Si₂H₄. But it is slightly smaller than the bond length of Si-Si single bond in a Si₂H₆ molecule. Subsequently, there may be some π -bonding character in the buckled Si=Si



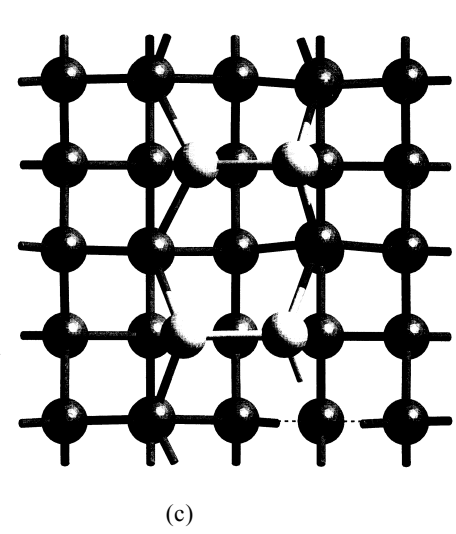


Fig. 1. The side and top view of relaxed buckled Si=Si dimer on Si(100) surface. (a) The parameters of bond length (Å) are reported. (b) The parameters of bond angle (°) are reported. (c) The top view of Si(100)-(2×2).

dimers. In addition, the reconstruction of Si(100) surface also leads to a slight contraction of the Si-Si distance between the first and second layers to around 2.330 Å. These results are in good agreement with other first principle calculated results. ¹⁴ To explore this buckled Si=Si dimers in more detail we present the contour of total valence charge density as shown in Fig. 2. The contour clearly shows an unevenly distributed valence charge density in the buckled Si=Si dimer bond region. Also we believe that this unevenly distributed valence charge density is one of main factors controlling the initial products of SiH_4 chemisorption onto a Si(100) surface, which will be discussed in a latter section.

Surface structure of Si(111)-(1×1)

Along the [111] direction of the silicon crystal one should expect to see a two-layer structure. Each Si atom in one of the two-layer has three bonds to connect with those in the other layer and one bond to another in a different two-layer. So when the surface along this direction is generated, each atom on the bulk terminated surface can have either one dangling bond or three dangling bonds. Again we found that the Si(111) surface when being generated will convert to Si(111)-(1×1) after relaxation. The first layer of Si atom on Si(111)-(1×1) surface having only one dangling bond is about 3.84 Å apart from the nearest dangling bonds, and its calculated relaxed geometry is shown in Fig. 3, and the corresponding structural pa-

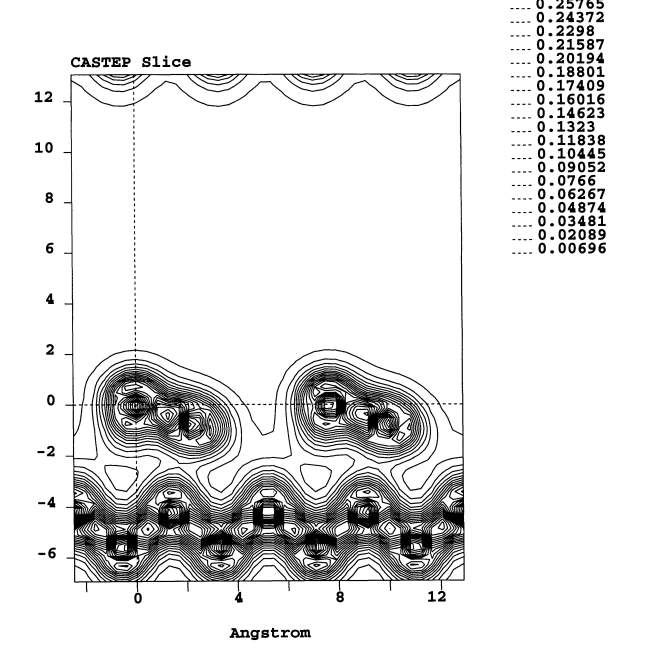
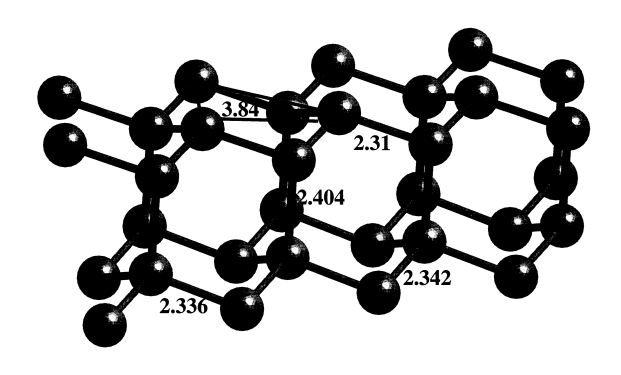
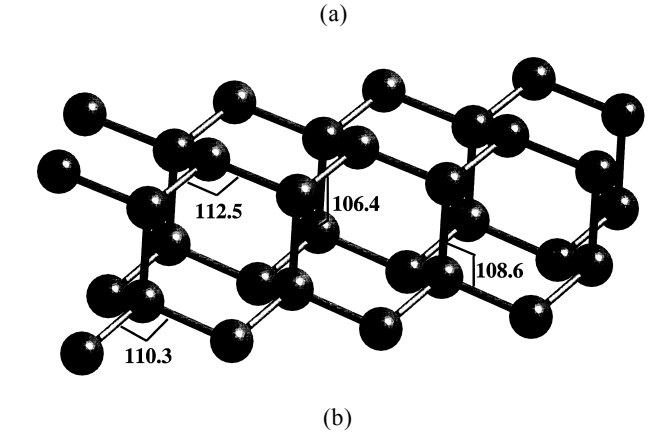


Fig. 2. Contours of total valence charge density (cutting through Si=Si) for buckled Si=Si dimer. Contour lines are drawn at intervals of 0.014 electrons/Å³ (From Ref. 21).

890





top layer Si atom

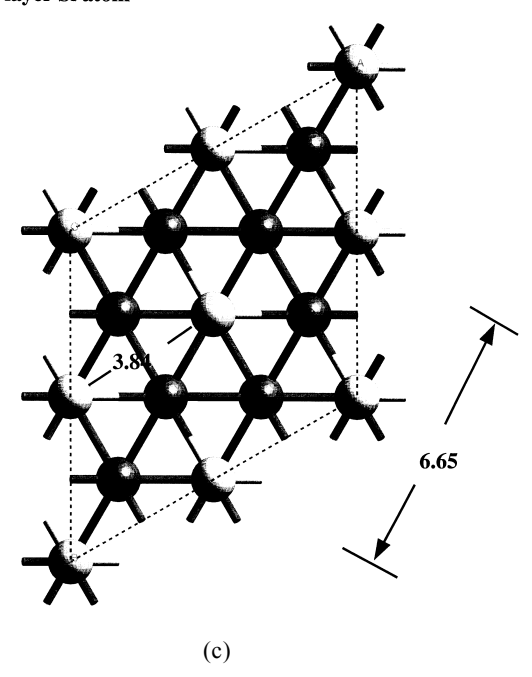


Fig. 3. The side and top view of relaxed Si(111)-(1×1) surface. (a) The parameters of bond length (Å) are reported. (b) The parameters of bond angle (°) are reported. (c) The top view of Si(111)-(1×1) surface.

rameters are reported. The calculated surface energy of Si(100)- (2×2) is nearly 1.89 eV/(per unit area) larger than that of Si(111)- (1×1) after relaxation. This is due to the longer separation (3.84 Å) between the nearest dangling bonds on the Si(111)- (1×1) surface thereby having the smaller interaction between the nearest neighboring dangling bonds to stabilize its surface structure. In consequence, this surface structure should provide different active sites for SiH_4 chemisorption in comparison with the Si(100)- (2×2) surface structure. The contour of total valence charge density of Si(111)- (1×1) is also shown in Fig. 4 to demonstrate the weaker interaction between dangling bonds on the Si(111)- (1×1) and the different surface environment of Si(111)- (1×1) compared to that of Si(100)- (2×2) .

It is well known according to Takayanagi DAS model that 1) the coverage of dangling bond on the Si(111)-(7×7) is about 0.387 and 2) the dangling bond on the adatom is about 4.4 Å away from and 1.5 Å above the dangling bond on the restatom on the Si(111)-(7×7). Based on the above description of Si(111)-(1×1) surface model we know that Si(111)-(7×7) \leftrightarrow Si(111)-(1×1) phase transition at $T_s > 800\,^{\circ}\text{C}$ will make the Si(111)-(7×7) surface lose all characteristics of the Si(111)-(1×1) surface mentioned earlier. Consequently, the sensitivity of reaction probability for dissociative chemisorption of SiH₄ onto Si(111)-(7×7) due to the Si(111)-(7×7) \leftrightarrow Si(111)-(1×1) phase transition was observed by experimental work of M. E.

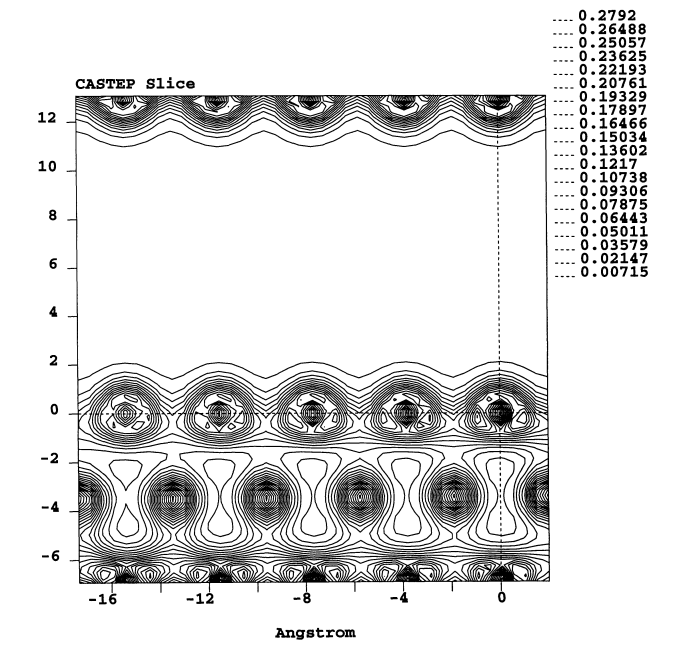
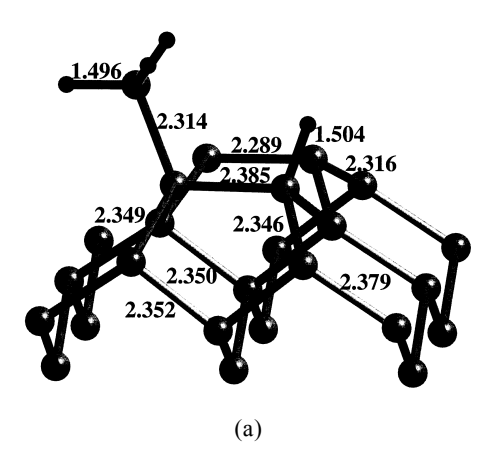


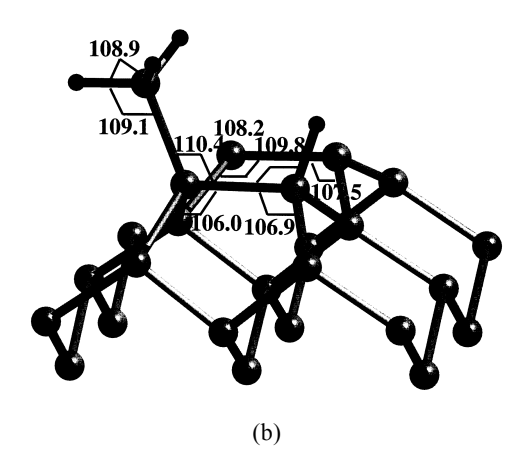
Fig. 4. Contours of total valence charge density (cutting through the dangling bonds) for Si(111)-(1 \times 1) surface. Contour lines are drawn at intervals of 0.014 electrons/Å³.

Jones et al. However, the corresponding reaction mechanisms still remain unclear. Therefore, it is our objective to first carry our DFT calculation studying the process of dissociative chemisorption of SiH₄ onto Si(111)-(1×1) leading to the final possible SiH₄ chemisorbed Si(111)-(1×1) surface. We then will compare our calculated results with experimental scanning tunneling microscopy (STM) results of D. Albertini et al. ²² who investigate room temperature dissociative chemisorption of SiH₄ onto Si(111)-(7×7) surface. Finally, we can rationalize the factors causing the increasing reaction probability for dissociative chemisorption of SiH₄ onto Si(111)-(7×7) due to Si(111)-(7×7) \leftrightarrow Si(111)-(1×1) phase transition at T_s > 800 °C which will be discussed in a later section.

SiH₄ chemisorbed Si(100)-(2 \times 2) surface: Si(100)-(2 \times 2) (SiH₃:H)

It has been suggested³ that during the chemisorption of SiH_4 onto Si(100)-(2×2) surface two new bonds are formed to the H and SiH₃ fragments from two dangling bonds on two adjacent surface Si atoms on the Si=Si dimer. Therefore, the dangling bonds are required for the initial chemisorption step. Also the qualitative reaction mechanism describing SiH₄ chemisorption on the Si(100)-(2×2) surface has been proposed.³ Here we will emphasize qualitatively the influence of electronic properties of the surface on the reaction mechanism of SiH₄ chemisorption onto our Si(100)-(2×2) surface model. To elaborate this we firstly realized that our calculated relaxed surface of Si(100)-(2×2) provides only two buckled asymmetric Si=Si dimers in parallel with each other as shown in Fig. 1. Therefore, we only expect to have SiH₄ species either chemisorbed on buckled-up Si atom or chemisorbed on buckled-down Si atom. Secondly, due to the formation of buckled asymmetric Si=Si dimers and the polarized electron pair toward H within the SiH₄ molecule we reasonably expect that during the process of dissociative chemisorption of SiH₄ onto the Si(100)-(2×2), the H atom within SiH₄ molecules will form the bond to buckled-down Si atom (electrophilic site) on the buckled Si=Si dimer and then the SiH₃ fragment which is nearest to the buckled-up Si atom will diffuse and form the bond to the buckled-up Si atom (nucleophilic site) on buckled Si=Si dimmer. 20,21 Consequently, two new bonds are formed to the H and SiH₃ fragments from two dangling bonds on two dimerized Si=Si atoms, i.e. Si(100)-(2×2)(SiH₃:H), as shown in Fig. 5, and corresponding structural parameters are reported. In order to obtain this energetic data we have to propose the reasonable initial structure of chemisorbed SiH₃ and H species on Si(100)- (2×1) surface based on our previous analysis of total valence charge density of buckled Si=Si dimer, then it is relaxed until the total energy minimum is reached in order to have our final calculated structure. The





top layer Si atom

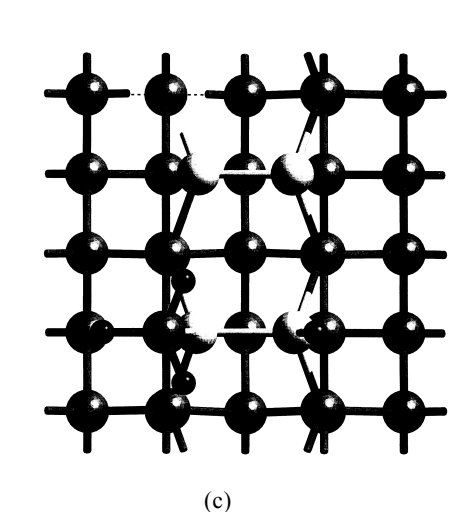


Fig. 5. The side and top view of SiH₄ chemisorbed on Si(100)-(2×2), i.e. Si(100)-(2×2)(SiH₃:H).

(a) The parameters of bond length (Å) are reported. (b) The parameters of bond angle (°) are reported. (c) The top view of Si(100)-(2×2)(SiH₃:H).

Table 2. The Calculated Chemisorption Energy (GGA) of SiH_4 Chemisorbed onto the Si(100)-(2×2), i.e. Si(100)-(2×2) (SiH_3 :H), and Si(111)-(1×1), i.e. Si(111)-(1×1)(SiH_2 :2H)

Species	$E_{chemisor.}(eV)$
Si(100)-(2×2)(SiH ₃ :H)	1.966
$Si(111)-(1\times1)(SiH_2:2H)$	2.669

calculated chemisorption energy, i.e. the total energy difference between SiH_4 above Si(100)- (2×2) and SiH_4 chemisorbed Si(100)- (2×2) , is reported in Table 2. Our calculated results strongly suggest that the chemisorption of SiH_4 onto the Si(100)- (2×2) is energetically favorable and it leads to stable structure of Si(100)- $(2\times2)(SiH_3:H)$.

SiH₄ chemisorbed Si(111)-(1×1) surface: Si(111)-(1×1) (SiH₂:2H)

It is intuitively known that the surface of Si(111)-(1 \times 1) with only one dangling bond on each Si atom of the first layer should provide different reactive sites for the chemisorption of SiH₄ onto the surface of Si(111)-(1 \times 1) in comparison with that of Si(111)-(7×7) and Si(100)-(2×2). However, the experimental work of M. E. Jones et al. is not able to propose the possible reaction mechanism for dissociative chemisorption of SiH₄ onto Si(111)-(1×1) leading to a SiH₄ chemisorbed Si(111)-(1×1) surface. Recently, scanning tunneling microscopy (STM) was used by D. Albertini et al.22 to investigate room temperature dissociative chemisorption of SiH₄ onto a Si(111)-(7×7) surface. They suggest that the reaction initially involves exclusively the corner holes and the adjacent Si adatoms of the Si(111)- (7×7) reconstruction, with preferential adsorption of SiH₃ groups in the corner holes and of H atoms on one of the adjacent corner adatoms. After higher SiH4 exposures the reactivity of the corner adatoms is significantly reduced; hydrogen adsorption occurs preferentially on the center adatoms. Therefore, they propose a model where the SiH₄ molecule decomposes near a restatom while two hydrogen atoms react with one of the three nearest adatom: one hydrogen atom saturates the adatom dangling bond and the other breaks the adatom backbond near the restatom and forms a dihydride silicon adatom. Accordingly, the silicon atom in the first layer which was originally attached to the adatom is now free. Then SiH₂ can bridge this atom and the neighboring restatom separated by 3.84 Å as shown in Fig. 6. Following the above description of forming the stable SiH₂ layer through bridging the Si atoms in the first layer separated by 3.84 Å we will focus our investigation only on the most possible path to initially form the chemisorbed SiH₂ species on Si(111)-(1 \times 1) surface. Based on our surface model of Si(111)- (1×1) one of the most probable paths for SiH₄ dissociative chemisorption onto the surface and leading to the forming of chemisorbed SiH₂ species on the surface of Si(111)-(2×2) is to allow SiH₄ to orient in such a way that 2H within the SiH₄ molecule will approach two dangling bonds on the Si(111)-(2×2) surface. When 2H within the SiH₄ molecule approach those sites the two dangling bonds will form the bonds to the 2H within the SiH₄ molecule. At the same time, the SiH₂ fragment will be dissociated from the SiH₄ molecule and diffuse toward and into the two nearest dangling bonds. Finally, two new bonds are formed to the SiH₂ from the two dangling bonds separated by 3.84 Å, i.e. Si(111)-(1×1)(SiH₂:2H), as shown in Fig. 7, and corresponding structural parameters are reported. By comparing our proposed reaction mechanisms with that of D. Albertini et al. using STM it is easily realized that additional breaking of the adatom backbond on Si(111)- (7×7) is needed to form the chemisorbed SiH₂ species on the Si(111)-(7×7) surface. We believe that this additional breaking of adatom backbond will greatly influence the reaction probability for dissociative chemisorption of SiH₄ onto a Si(111)-(7×7) surface when compared to that for dissociative chemisorption of SiH₄ onto a Si(111)- (1×1) surface.

Our calculated chemisorption energy with GGA for the formation of chemisorbed SiH₂ and 2H species on the Si(111)- (1×1) surface, i.e. Si(111)- (1×1) (SiH_2 :2H) is about 0.803 eV/(per SiH₄) more favorable than the formation of chemisorbed SiH₃ and H species on the Si(100)-(2×2) surface, i.e. Si(100)- $(2\times2)(SiH_3:H)$, as shown in Table 2. This difference in chemisorption energy at different Si surfaces indicates that SiH₄ is energetically more favourable to form Si(111)- $(1\times1)(SiH_2:2H)$ rather than $Si(100)-(2\times2)(SiH_3:H)$. Finally, what are the main factors dictating the distinct increase in reaction probability for dissociative chemisorption of SiH₄ onto Si(111)- (7×7) due to Si(111)- $(7\times7) \leftrightarrow Si(111)$ - (1×1) phase transition at $T_s > 800$ °C. First of all we realized that there is a significant increase in dangling bond density due to the Si(111)- $(7\times7) \leftrightarrow Si(111)$ - (1×1) phase transition at $T_s > 800$ °C. Secondly, as mentioned above, the proposed mechanism for dissociative chemisorption of SiH₄ onto Si(111)-(7×7) by D. Albertini et al. using STM involves additional breaking of

Fig. 6. The sketch of silane adsorption mechanism on Si(111)- (7×7) proposed by D. Albertini et al.

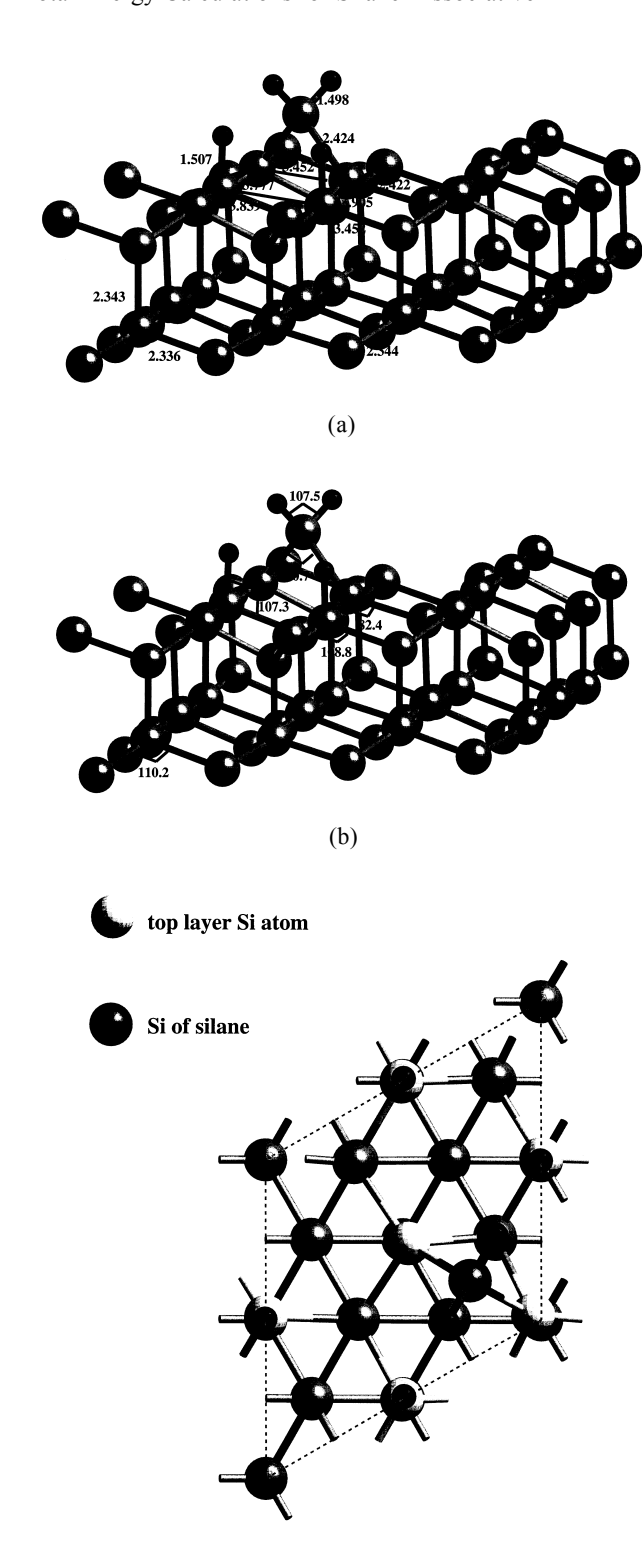


Fig. 7. The side and top view of SiH_4 chemisorbed on Si(111)- (1×1) , i.e. Si(111)- $(1\times1)(SiH_2:2H)$. (a) The parameters of bond length (Å) are reported. (b) The parameters of bond angle (°) are reported. (c) The top view of Si(111)- $(1\times1)(SiH_2:2H)$.

(c)

the adatom backbond compared to our proposed reaction mechanism for dossociative chemisorption of SiH_4 onto Si(111)- (1×1) . In consequence, we should expect that there is a higher reaction probability for dissociative chemisorption of SiH_4 onto Si(111)- (1×1) .

CONCLUSIONS

By combining both density functional theory and pseudopotential total energy calculations technique we are able to investigate qualitatively the possible reaction mechanisms describing dissociative chemisorption of SiH₄ onto both Si(100)-(2×2) surface and Si(111)-(1×1). Our collectively calculated results suggest that 1) the relaxation of the Si(100) surface leading to the formation of buckled Si=Si dimer, i.e. Si(100)- (2×2) , is crucial for reasoning the formation of chemisorbed SiH₃ and H species on this surface, i.e. Si(100)-(2×2)(SiH₃:H) and 2) the increase of dangling bond density and the absence of adatom backbond breaking on the Si(111)- (1×1) are two of the major factors governing the distinct increase in reaction probability for dissociative chemisorption of SiH₄ onto Si(111)-(7×7) due to Si(111)-(7×7) \leftrightarrow Si(111)-(1×1) phase transition at $T_s > 800$ °C. Finally, our calculated results provide supplemental evidence in terms of atomic arrangement and corresponding energetic data to help rationalize the possible reaction mechanisms of dissociative chemisorption of SiH₄ onto both Si(100)-(2×1) and Si(111)-(7×7) $(T_s > 800 \text{ °C})$ surfaces, and to corroborate studies by S. M. Gate et al. and M. E. Jones et al., respectively.

ACKNOWLEDGMENTS

The authors would like to thank the National Science Council in Taiwan (Grant No. 86-2113-M-032-012 and 87-2113-M-032-005) for financial support and the National Center for High Performance Computing and Tamkang University in Taiwan for use of computational facilities.

REFERENCES

- Waltenburg, H. N.; Yates, Jr. J. T. Chem. Rev. 1995, 95, 1589; Gates, S. M. Chem. Rev. 1995, 96, 1519.
- Ekerdt, J. G.; Sun, Y.-M.; Szabo, A.; Szulczewski, G. J.; White, J. M. Chem. Rev. 1996, 96, 1499.
- 3. Gates, S. M.; Greenlief, C. M.; Beach, D. B. *J. Chem. Phys.* **1990**, *93*, 7493.

- Gates, S. M.; Greenlief, C. M.; Beach, D. B.; Holbert, P. A. J. Chem Phys. 1990, 92, 3144.
- Jones, M. E.; Xia, L.-Q.; Maity, N.; Engstrom, J. R. Chem. Phys. Letter 1995, 325, L441.
- 6. Konecny, R.; Doren, D. J. J. Chem. Phys. 1997, 106, 2426.
- Weakliem, P. C.; Carter, E. A. J. Chem. Phys. 1993, 98, 737; Radekr, M. R.; Carter, E. A. Surface Sci. 1996, 355, L28; Wu, C. J.; Carter, E. A. Chem. Phys. Lett. 1991, 185, 172.
- 8. Ihm, J. Rep. Prog. Phys. 1988, 51, 105.
- Teter, M. P.; Payne, M.. C.; Allan, D. C. *Phys. Rev. B* 1989, 40, 12255.
- Payne, M. C.; Teter, M. P.; Allan, D. C.; Arias, T. A.;
 Joannopoulos, J. D. Rev. Mod. Phys. 1992, 64, 1045.
- 11. Monkhorst, H. J.; Pack, J. D. Phys. Rev. B 1976, 13, 5188.
- 12. Kleinman, L.; Bylander, D. M. *Phys. Rev. Lett.* **1982**, *48*, 1425.
- Rappe, A. M.; Rabe, K. M.; Kaxiras, E.; Joannopoulos, J. D. *Phys. Rev. B* 1990, 41, 1227; Lin, J. S.; Qteish, A.; Payne, M. C.; Heine, V. *Phys. Rev. B* 1993, 47, 4174.

- Kruger, P.; Pollmann, J. *Phys. Rev. Lett.* **1995**, *74*, 1155.
 Milman, V.; Jesson, D. E.; Pennycook, S. J.; Payne, M. C.;
 Lee, M. H.; Stich, I. *Phys. Rev. B* **1994**, *50*, 2663.
- Wang, J.; Arias, T. A.; Joannopoulos, J. D. *Phys. Rev. B* 1993, 47, 10497; Ihara, S.; Ho, S. L.; Uda, T.; Hirao, M. *Phys. Rev. Lett.* 1990, 65, 1909.
- 16. Takayanangi, K.; Tanishiro, Y.; Takahashi, M.; Takahashi, S. *J. Vac. Sci. Technol. A* **1985**, *3*, 1502.
- 17. Stich, I.; Payne, M. C.; King-Smith, R. D.; Lin, J. S.; Clarke, L. J. *Phys. Rev. Lett.* **1992**, *68*, 1351.
- 18. Perdew, J. P. in *Electronic Structure of Solids*; Ziesche, P.; Eschrig, H., Eds.; Akademie Verlag: Berlin, **1991**; Perdew, J. P.; Wang, J. (unpublished).
- 19. Wolkow, R. A. Phys. Rev. Lett. 1992, 68, 2636.
- 20. Lin, J. S.; Kuo, Y. T. Thin Solid Film (in press).
- 21. Lin, J. S.; Kuo, Y. T.; Lee, M. H.; Lee, K. H.; Chen, J. C. *Theochem* **2000**, *496*, 163.
- 22. Albertini, D.; Thibaudau, F.; Masson L.; Salvan, F. *Surf. Sci.* **1992**, *350*, L216.